Receptor Cross-Linking on Human Plasmacytoid Dendritic Cells Leads to the Regulation of IFN-α Production[1]

Stacey L. Fanning,*† Thaddeus C. George,‡ Di Feng,*† Steven B. Feldman,* Nicholas J. Megjugorac,*† Alexander G. Izaguirre,*† and Patricia Fitzgerald-Bocarsly[2]*†

Plasmacytoid dendritic cells (PDC) are the natural type I IFN-producing cells that produce large amounts of IFN-α in response to viral stimulation. During attempts to isolate PDC from human PBMC, we observed that cross-linking a variety of cell surface receptors, including blood DC Ag (BDCA)-2, BDCA-4, CD4, or CD123 with Abs and immunobeads on PDC leads to inhibition of IFN-α production in response to HSV. To understand the mechanisms involved, a number of parameters were investigated. Cross-linking did not inhibit endocytosis of soluble Ag by PDC. Flow cytometry for annexin V and activated caspase-3 indicated that PDC are not undergoing apoptosis after receptor cross-linking. Cross-linking of CD123, but not the other receptors, caused the up-regulation of costimulatory molecules CD80 and CD86, as well as the down-regulation of CD62L, indicating PDC maturation. Thus, anti-CD123 Ab may be acting similar to the natural ligand, IL-3. Anti-phosphotyrosine Ab, as well as Ab to the IFN regulatory factor, IRF-7, was used in intracellular flow cytometry to elucidate the signaling pathways involved. Tyrosine phosphorylation occurred after cross-linking BDCA-2 and BDCA-4, but not CD4. Cross-linking did not affect IRF-7 levels in PDC, however, cross-linking BDCA-2, BDCA-4, and CD4, but not CD123, inhibited the ability of IRF-7 to translocate to the nucleus. Taken together, these results suggest that cross-linking BDCA-2, BDCA-4, and CD4 on PDC regulates IFN-α production at the level of IRF-7, while the decrease in IFN-α production after CD123 cross-linking is due to stimulation of the IL-3R and induction of PDC maturation. *The Journal of Immunology,* **2006, 177: 5829–5839.**

Plasmacytoid dendritic cells (PDC)[3] are a rare and unique population of cells that are major players in directing immune responses. Initially, PDC were recognized for their role in innate antiviral immunity. However, it is now being revealed that these cells are involved in several aspects of immunity including directing cell trafficking via chemokine production (1, 2), acting as accessory cells in B cell Ab production (3, 4), and inducing Th1, Th2, or T_{reg} responses, depending on the nature of the stimulation (5–7). Perhaps the best studied aspect of PDC function is their ability to produce the antiviral cytokine IFN-α. PDC are known to be identical with the natural IFN-producing cells (IPC) in peripheral blood (8) and produce large quantities of IFN-α (as much as 2–5 pg/cell) in response to enveloped viruses, such as HSV, some bacteria, CpG-containing DNA, and imidazoquinolines (8–16). The PDC can be phenotypically distinguished from other PBMC by its cell surface markers; PDC are lineage negative, HLA-DR$^+$, CD11c$^-$, and CD123^{bright} (17). PDC also express the newly characterized cell surface markers, blood DC Ag (BDCA)-2 and BDCA-4 (18). BDCA-2 is a C-type lectin involved in endocytosis. Dzionek et al. (19) have shown that anti-BDCA-2 mAb is rapidly internalized by PDC and efficiently presented to T cells, suggesting a role for this receptor in Ag capture. BDCA-4 has recently been shown to be identical with neuropilin-1 (NP-1), a neuronal receptor for axon guidance factors and a coreceptor for vascular endothelial growth factor (VEGF) (20). Although its role on PDC has yet to be elucidated, one report suggests that NP-1 might be involved in naive T cell/DC interaction (21).

PDC typically comprise only 0.2–0.5% of all PBMC (22, 23). Human PDC can be purified from PBMC by using magnetic bead separation techniques. In these separations, PBMC are labeled with microbead-conjugated CD3, CD16, and CD11b Abs to deplete T cells, NK cells, monocytes, and myeloid DCs, respectively. When run through a magnetic isolation column, unlabeled cells are collected as an untouched, negatively selected population. These cells, typically consisting of 60% PDC, are then labeled with microbead-conjugated anti-CD4 Ab to positively select the PDC. Alternatively, PDC can be isolated from PBMC in one positive selection step using either anti-BDCA-2 or anti-BDCA-4 microbeads. After positive selection, the cell population typically consists of >95% PDC.

During our attempts to isolate a pure population of PDC from PBMC using a magnetic bead cell isolation kit, we observed that positively selecting PDC leads to the inhibition of IFN-α production by these cells in response to viral stimulation. This led us to hypothesize that cross-linking cell surface receptors on the PDC was interfering with its ability to produce IFN-α. Similarly, Dzionek et al. (19) have reported that BDCA-2 ligation with anti-BDCA-2 Ab leads to an inhibition in IFN-α production in response to influenza virus, while Kerkmann et al. (24) have shown that BDCA-2 cross-linking results in an inhibition in CpG DNA-induced IFN-α production. The exact mechanism by which cross-linking cell surface receptors on PDC leads to this inhibition in

*New Jersey Medical School and †Graduate School of Biomedical Sciences, University of Medicine and Dentistry of New Jersey, Newark, NJ 07103; and ‡Amnis, Seattle, WA 98121

Received for publication October 17, 2005. Accepted for publication August 14, 2006.

The costs of publication of this article were defrayed in part by the payment of page charges. This article must therefore be hereby marked *advertisement* in accordance with 18 U.S.C. Section 1734 solely to indicate this fact.

[1] This work was supported by National Institutes of Health Grants AI26806 (to P.F.-B.) and a fellowship from the Graduate School of Biomedical Sciences, University of Medicine and Dentistry of New Jersey (to S.L.F.).

[2] Address correspondence and reprint requests to Dr. Patricia Fitzgerald-Bocarsly, Department of Pathology and Laboratory Medicine, New Jersey Medical School, University of Medicine and Dentistry of New Jersey, 185 South Orange Avenue, Newark, NJ 07103. E-mail address: bocarsly@umdnj.edu

[3] Abbreviations used in this paper: PDC, plasmacytoid dendritic cell; BDCA, blood DC Ag; NP-1, neuropilin-1; VEGF, vascular endothelial growth factor; IRF, IFN regulatory factor; MOI, multiplicity of infection; MDDC, monocyte-derived DC; 7-AAD, 7-aminoactinomycin D; IPC, IFN-α-producing cell; MFI, mean fluorescence intensity; SLE, systemic lupus erythematosus; IIF, IFN-α-inducing factor.

0022-1767/06/$02.00

IFN-α production is unknown, and may be important to understanding how IFN-α production is regulated in these cells. Therefore, our aim was to determine the mechanism by which cross-linking receptors on the surface of PDC leads to the inhibition of IFN-α production in response to viral stimulation.

In the current study, we demonstrate that cross-linking a wide variety of cell surface receptors on PDC, including CD4, BDCA-2, BDCA-4, and CD123, leads to the inhibition of IFN-α production in response to viral stimulation. We examined several potential mechanisms by which cross-linking cell surface receptors on PDC could lead to the down-regulation of IFN-α production. These include inhibition of interaction with or uptake of virus, PDC apoptosis, PDC maturation, or regulation of the IFN-α induction pathway. In this study, we show that the cross-linking of different cell surface markers may not be working by the same mechanism to inhibit IFN-α production. The data presented shows that the inhibition of IFN-α production that results from CD123 cross-linking is due to the maturation of PDC, as indicated by their up-regulation of costimulatory molecules. In contrast, the inhibition of IFN-α seen with BDCA-2, BDCA-4, and CD4 cross-linking is likely due to regulation of IFN-α production at the level of IRF-7.

Materials and Methods

Viruses and cell lines

HSV-1 strain 2931 (originally obtained from Dr. C. Lopez, then of the Sloan-Kettering Institute for Cancer Research (New York, NY)) and vesicular stomatitis virus (originally obtained from Dr. N. Ponzio (New Jersey Medical School, Newark, NJ)) were grown and titrated by plaque-forming assay in VERO cells (American Type Culture Collection) as previously described (25). The primary fibroblast cell line, GM-0459A (National Institute of General Medicine Sciences Human Genetic Mutant Cell Line Repository), which is trisomic for chromosome 21, was grown in DMEM (JHR Biosciences) supplemented with 15% FCS (HyClone), 2 mM L-glutamine, 100 U/ml penicillin, and 100 μg/ml streptomycin.

Cell preparations

PBMC were freshly isolated by Ficoll-Hypaque density centrifugation (Lymphoprep; Accurate Chemical and Scientific) of heparinized blood from healthy donors. Human PBMC studies were approved by the Institutional Review Board of the New Jersey Medical School. PBMC were washed twice with HBSS (Invitrogen Life Technologies) and resuspended in RPMI 1640 medium (Invitrogen Life Technologies) containing 10% FCS, 2 mM L-glutamine, 100 U/ml penicillin, 100 μg/ml streptomycin, and 25 mM HEPES (RPMI 1640, 10%). Enriched PDC were obtained from PBMC by negative selection using a modification of the Magnetic Blood Dendritic Cell Isolation kit I from Miltenyi Biotec. PBMC were washed and resuspended in MACS buffer (1× PBS (Invitrogen Life Technologies) with 0.5% BSA and 2 mM EDTA). PBMC were depleted of T cells, monocytes, and NK cells by labeling with hapten-conjugated murine Abs against CD3, CD11b, and CD16. Cells were incubated at 4°C for 10 min and washed twice in MACS buffer. This was followed by the addition of anti-hapten microbeads, as well as anti-glycophorin A and anti-CD19 microbeads, to additionally deplete RBC and B cells, respectively. Alternatively, PDC were enriched from PBMC using the Plasmacytoid Dendritic Cell Isolation kit (Miltenyi Biotec) as per the manufacturer's instructions. The microbead-labeled cell suspensions were run through an LD-negative selection column. The flow-through was collected as an enriched PDC population. PDC were evaluated for purity using flow cytometry. Typically, the negatively enriched population was found to contain 60% PDC using the Magnetic Blood Dendritic Cell Isolation kit I and >80% PDC using the Plasmacytoid Dendritic Cell Isolation kit as defined by cells that were HLA-DR$^+$, Lin$^-$, CD11c$^-$, and CD123$^+$ by flow cytometry, as described below.

Receptor cross-linking on PDC

CD4 and BDCA-4 on PDC were cross-linked using anti-CD4 and anti-BDCA-4 microbeads, respectively (Miltenyi Biotec). Briefly, PBMC were washed and resuspended in MACS buffer. Anti-CD4 or anti-BDCA-4 microbeads (25 μl/1 $\times$ 10^7 cells) were added and cells were incubated at 4°C for 15 min. BDCA-2 was cross-linked on PDC using either biotinylated anti-BDCA-2 Ab (25 μl/1 $\times$ 10^7 cells) or unlabeled anti-BDCA-2 Ab (10 μg/1 $\times$ 10^7 cells). PBMC were incubated with primary Ab for 10 min. After washing in MACS buffer, anti-biotin microbeads (40 μl/1 $\times$ 10^7 cells) or rat anti-mouse IgG1 microbeads (20 μl/1 $\times$ 10^7 cells) (Miltenyi Biotec) were added and incubated for 15 min at 4°C. For CD123 cross-linking, anti-CD123 Ab (2 ng/1 $\times$ 10^6 cells) (BD Pharmingen) was added to PBMC, incubated for 20 min at 4°C, and washed in MACS buffer, followed by incubation with rat anti-mouse IgG1 conjugated microbeads (Miltenyi Biotec) for 15 min at 4°C. Mouse IgG1 isotype control Ab (BD Pharmingen) with anti-IgG1 microbeads was used as a negative control for cross-linking. Following cross-linking, PBMC were washed and resuspended in RPMI 1640, 10%.

IFN bioassay

IFN bioassays were performed using a cytopathic effect reduction assay with GM-0459A (GM) cells infected with vesicular stomatitis virus as the challenging virus as previously described (25). An IFN-α reference standard (standard G-023-901-527; National Institute of Allergy and Infectious Disease, Bethesda, MD) was used at 100 IU/ml.

ELISPOT assay

Millititer HA 96-well Multiscreen plates (no. MAHAN4550; Millipore) were coated with the IgG fraction of ammonium sulfate-precipitated bovine polyclonal anti-human IFN-α Ab (100 μg/ml in 1× PBS; GlaxoSmithKline) for at least 5 h at room temperature. Receptor cross-linking was performed using the following mAbs, all at a concentration of 2 ng/1 $\times$ 10^6 cells: anti-BDCA-2 mAb and anti-BDCA-4 mAb (Miltenyi Biotec), anti-CD4 mAb (SIM4), anti-CD123 mAb, anti-CD62L mAb, and anti-MHC class I mAb (BD Pharmingen). Cells were incubated with primary Ab for 20 min at 4°C and in the case of secondary cross-linking were washed and then incubated with rat anti-mouse IgG1 microbeads (Miltenyi Biotec) for 15 min at 4°C. PBMC (1 $\times$ 10^6 cells/ml) stimulated with HSV for 6 h at 37°C were plated in triplicate (1 $\times$ 10^5 cells/well) and incubated overnight at 37°C. The following day, the plate was washed with PBS and PBS-Tween (Sigma-Aldrich). Murine monoclonal 293 anti-human IFN-α Ab (1.1 μg/ml in 3% BSA in PBS) (provided by G. Alm, Swedish University of Agricultural Sciences, Uppsala, Sweden) was added and the plate was incubated at room temperature for 2 h. After washing, goat anti-mouse IgG HRP conjugate (diluted 1/750 in 3% BSA in PBS; The Jackson Laboratory) was added and incubated for 1 h at 37°C. The plate was developed using 3,3′-diaminobenzidine tetrahydrochloride (Sigma-Aldrich) with 30% H_2O_2. Spots were enumerated using a dissecting microscope.

Flow cytometry

PMBC were stimulated as described in each experiment. After washing with 0.1% BSA in PBS, cells were resuspended in PBS containing 5% heat-inactivated human serum and incubated with fluorochrome-conjugated Abs at 4°C for 20 min. The cells were then washed with PBS and fixed in 1% paraformaldehyde (Fisher Scientific) in PBS. Abs used were as follows: anti-IgG2a, IgG1 (DakoCytomation); CD80, CD86 (BD Pharmingen); CD62L, CD11c, CD123, and HLA-DR (BD Biosciences); BDCA-2 and BDCA-4 (Miltenyi Biotec). Data were acquired using a FACSCalibur flow cytometer and analyzed using CellQuest software (BD Biosciences).

Intracellular flow cytometry

PBMC (2 $\times$ 10^6 cells/ml) were stimulated with 10,000 IU/ml recombinant human IFN-α2b (Schering-Plough) or HSV-1 strain 2931 (multiplicity of infection (MOI) = 1) for 4 h at 37°C in 5% CO_2. Brefeldin A (5 μg/ml; Sigma-Aldrich) was added and incubation continued for an additional 2 h. Cells were washed with 0.1% BSA (Sigma-Aldrich) in 1× PBS (Invitrogen Life Technologies), and stained for PDC-specific cell surface markers as described above. Cells were fixed with 1% paraformaldehyde and stored at 4°C overnight. The following day, cells were permeabilized with 0.5% saponin (Sigma-Aldrich) in 1× PBS with 0.2% FCS and stained for intracellular IFN-α or phosphorylated tyrosine using biotinylated mouse anti-human IFN-α Ab clone MMHA-2 (50 ng; PBL) (Ab was purchased unconjugated and was biotinylated using *N*-hydroxysuccinimide biotin (Sigma-Aldrich)) or biotinylated mouse anti-phosphotyrosine Ab (5 ng; Santa Cruz Biotechnology), respectively, followed by secondary staining with streptavidin-conjugated quantum red (Sigma-Aldrich). For IFN regulatory factor (IRF)-7, PBMC were stained with rabbit anti-human IRF-7 Ab (400 ng; Santa Cruz Biotechnology) followed by FITC-labeled goat anti-rabbit IgG secondary Ab (BD Pharmingen) as previously described (26). For activated caspase-3, rabbit anti-human activated caspase-3 Ab conjugated to FITC (20 μl/1 $\times$ 10^6 cells; BD Pharmingen) was added after cell permeabilization and incubated for 30 min at room temperature. After staining, cells were washed and fixed in 1% paraformaldehyde in PBS.

Data were acquired using a FACSCalibur flow cytometer and analyzed using CellQuest software.

Generation of monocyte-derived DCs (MDDC)

MDDC were prepared by culture of plastic-adherent mononuclear cells in RPMI 1640 containing 1% autologous plasma, 500 IU/ml IL-4 (R&D Systems) and 1000 IU/ml GM-CSF (Sargramostim-Leukine; Immunex). The cells were fed with IL-4 and GM-CSF-containing medium on days 2, 4, and 6 by 50% medium exchange and nonadherent cells were collected as MDDC on day 7 and evaluated by flow cytometry.

FITC-dextran uptake assays

PBMC (1×10^6 in 100 μl) were equilibrated at 37°C for 5 min. FITC-conjugated dextran (Sigma-Aldrich) was added at a final concentration of 1 mg/ml and cells were incubated at 37°C for the time points indicated in the figure. For the negative control, cells were incubated with FITC-dextran on ice. Cells were washed three times in cold PBS with 0.01% NaN_3 followed by surface staining with anti-CD123 PE and anti-HLA-DR allophycocyanin or anti-BDCA-2 PE and anti-BDCA-4 allophycocyanin to gate on PDC. Cells were fixed with 1% paraformaldehyde and analyzed by flow cytometry.

Annexin V staining

PBMC were cross-linked and incubated at 37°C for 6 h. As a positive control for apoptosis, PBMC were heated at 50°C for 10 min. Cells were surfaced stained with CD123 PE and HLA-DR allophycocyanin or BDCA-2 PE and BDCA-4 allophycocyanin to gate on PDC, followed by staining using the Annexin V FITC apoptosis kit (BD Pharmingen) in combination with 7-aminoactinomycin D (7-AAD; 15 μg/ml final concentration) (Sigma-Aldrich). Cells were immediately acquired using a FACSCalibur flow cytometer and analyzed using CellQuest software.

Fluorescent microscopy

PDC were enriched from PBMC by negative selection as described above. Enriched PDC were cross-linked with anti-CD4 microbeads and incubated with HSV-1 at an MOI of 1 for 3 h at 37°C. Cells were surface stained with anti-BDCA-2 PE and fixed in 1% paraformaldehyde overnight at 4°C. The following day, the cells were adhered to slides using the Shandon Cytospin 2. Cells were permeabilized with 0.2% Triton X-100 in PBS and stained for IRF-7 using rabbit anti-human IRF-7 Ab (4 ng/ml) or polyclonal rabbit IgG as an isotype control (Santa Cruz Biotechnology) followed by FITC-labeled goat anti-rabbit IgG secondary Ab (1/20 dilution; BD Pharmingen). Slides were washed and nuclei were stained using 4′6′-diamidino-2-phenylindole (50 ng/ml; Sigma-Aldrich). Slides were viewed under fluorescence with an Olympus fluorescence microscope with digital image capture.

Determination of nuclear translocation using the ImageStream

PDC were enriched from PBMC by negative selection as described above. PBMC were added back to the enriched PDC to bring the number of cells to $2–5 \times 10^6$ per condition. Cells were cross-linked as described above and stimulated with HSV-1 (MOI = 1) for 3 h at 37°C. After incubation, cells were surface stained with both anti-BDCA-2 PE and anti-BDCA-4 PE Abs, fixed in 1% paraformaldehyde and stored at 4°C overnight. The following day, samples were permeabilized with 0.1% Triton X in 1× PBS and incubated with anti-IRF-7 Ab as described above for intracellular flow cytometry. For secondary Ab, chicken anti-rabbit Ig Alexa Fluor 488 (Molecular Probes) (10 ng/μl) was added and cells were incubated for 30 min at room temperature. Following washing, cells were fixed in 1% paraformaldehyde and shipped overnight on ice to Amnis. Nuclei were stained with 7-AAD (50 μg/ml) immediately before acquisition. Samples were acquired using the ImageStream imaging flow cytometer and analyzed using IDEAS software (Amnis) as recently described (27). In-focus cells were identified by gating on 7-AAD-positive events with high 7-AAD aspect ratios (width to height, measure of circularity) and high nuclear contrast (as measured by the Gradient Max feature). PDC were identified from this population based on their IRF-7^{bright} staining and BDCA-2- and BDCA-4-positive phenotype. Nuclear localization of IRF-7 within PDC was then measured using the similarity score, which quantifies the correlation of pixel values of the 7-AAD and IRF-7 images on a per cell basis (27). Positive values signify similarity between nuclear and IRF-7 staining indicating nuclear translocation, while negative values signify antisimilarity indicating cytoplasmic localization.

Statistical analysis

Data were analyzed using the Statview statistics program. Significant differences between groups were determined by ANOVA using the Scheffe's test, with values of $p < 0.05$ considered significant. Statistics for IRF-7 nuclear translocation as determined by the ImageStream were generated using the one-sided Mann-Whitney U test to compare median similarity scores between untreated and treated groups. This test is useful for detecting small shifts of known sign between unpaired sample measurements, when the measurements are not expected to be normally distributed.

Results

Cross-linking receptors on the surface of PDC leads to the inhibition of IFN-α in response to HSV

In attempts to isolate PDC from PBMC using the Magnetic Blood Dendritic Cell Isolation kit I from Miltenyi Biotec, we observed that when PDC were positively selected using anti-CD4 Ab-conjugated microbeads, these positively selected PDC had reduced capacity to produce IFN-α in response to stimulation with HSV than would be predicted by the relative-fold enrichment (data not shown). In contrast, negatively selected PDC (40–60% purity) obtained by depletion of T cells, B cells, monocytes, and NK cells produced expected levels of IFN-α based on the level of enrichment. Likewise, we earlier demonstrated that very high levels of IFN-α activity on a per cell basis were obtained following Percoll density gradient separation (28). We hypothesized that the binding of microbead-conjugated Ab to CD4 on PDC was causing the decreased ability to produce IFN-α by cross-linking this cell surface receptor. We further investigated the phenomenon using Abs or Ab-conjugated microbeads to other PDC cell surface markers. BDCA-2, BDCA-4, CD4, CD123, CD62L, or MHC class I were cross-linked on PBMC using either Ab alone or Ab followed by anti-IgG1 microbeads. After incubation with Abs, cells were thoroughly washed to exclude any effect of NaN_3 in the Ab preparations. As a control, PBMC were incubated with anti-IgG1 microbeads in the absence of a primary Ab. PBMC were stimulated with HSV for 6 h and the frequency of IFN-α producing cells (IPC) was measured by ELISPOT assay. Fig. 1 shows the percent inhibition in frequency of IPC after cross-linking with Ab alone or Ab plus anti-IgG1 microbeads. Although cross-linking with Ab alone led to some inhibition in IPC frequency (mean inhibition 27%), cross-linking with Ab and microbeads caused an even greater inhibition (mean inhibition 73%). To ensure that the observed effects were due to the direct action of the cross-linking on PDC and not indirect effects on other cell populations within the PBMC, PDC were first enriched by negative selection (>80% PDC) and then BDCA-2 or CD4 were cross-linked as described. After overnight stimulation with HSV, supernatants were collected and IFN bioassay was performed. The results show that cross-linking of highly enriched PDC led to decreased IFN-α production and suggests that the effect seen is independent of other cell populations (Fig. 1*B*).

We next measured IFN-α production in cross-linked PDC using intracellular flow cytometry. BDCA-2, BDCA-4, CD4, and CD123 were cross-linked on PBMC using Ab and microbeads. The PBMC were then stimulated with HSV (MOI = 1) for 6 h at 37°C. Cells were surface stained for PDC-defining markers CD123 PE and HLA-DR allophycocyanin (29, 30) or BDCA-2 PE and BDCA-4 allophycocyanin, and intracellular flow cytometry for IFN-α was performed. As shown in Fig. 2, *A* and *B*, the percent of PDC expressing IFN-α was reduced after cross-linking each of these cell surface receptors. Although BDCA-2, BDCA-4, and CD123 cross-linking lead to reduced IFN-α, CD4 cross-linking almost completely abolished the ability of PDC to produce IFN-α in response to stimulation with HSV. The addition of an IgG isotype control Ab, followed by

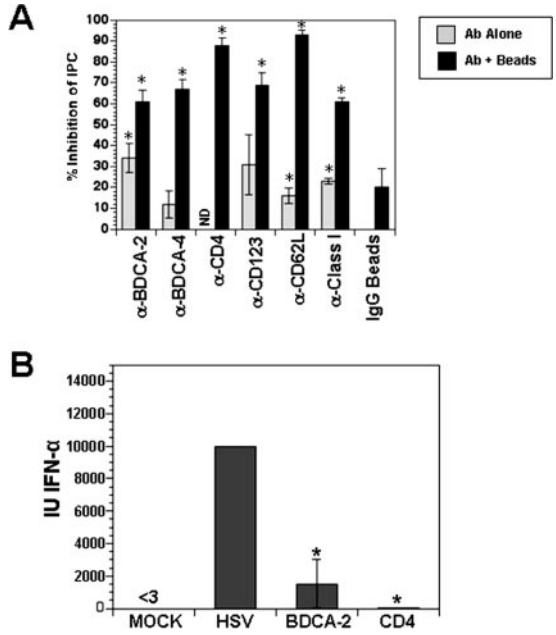

FIGURE 1. Cross-linking cell surface receptors on PDC with either Ab alone or Ab and anti-IgG1 microbeads leads to a decrease in IFN-α-producing cells and total IFN-α in response to HSV. *A*, PBMC were incubated with Abs specific for BDCA-2, BDCA-4, CD4, CD123, CD62L, or MHC class I alone (▨) or with secondary cross-linking with anti-IgG1 microbeads (■). PBMC (1×10^6/ml) were stimulated with HSV-1 (MOI = 1) for 6 h. Frequency of IFN-α-producing cells was determined by ELISPOT assay. Results are shown as percent inhibition of IFN-α-producing cells, with the non-cross-linked cells having 0% inhibition (no cross-linking = 8.8 ± 2.1 IPC/1×10^4 PBMC). The mean percent inhibition ± SEM of $n = 3$ independent experiments are shown. ∗, Significant differences ($p < 0.05$) between no cross-linking and cross-linked cells. *B*, PDC were enriched from PBMC by negative selection. PDC were cross-linked using either BDCA-2 Ab followed by IgG microbeads, or CD4 microbeads. Cells were stimulated with HSV-1 at an MOI of 1. After overnight incubation at 37°C, supernatants were collected and IFN bioassay was performed as described in *Materials and Methods*. IFN-α production (IU) ± SEM of $n = 3$ independent experiments is shown. ∗, Significant differences ($p < 0.05$) between no cross-linking and cross-linked cells.

cross-linking with anti-IgG1 microbeads, did not lead to any significant decrease in IFN-α production showing the observed result is due to specific Ab binding. IFN-α bioassay and ELISPOT show that both the total amount of IFN-α released (Fig. 2*C*) and the frequency of cells producing IFN-α (Fig. 2*D*), respectively, were reduced by cell surface receptor cross-linking. To ensure that this phenomenon was specific to PDC, monocytes were cross-linked with Ab-conjugated microbeads for CD11c, CD4, CD62L, CD16, and CD14, all of which are present on monocytes, and stimulated with Sendai virus. Monocytes were gated by surface expression of CD14 and IFN-α production was measured by intracellular flow cytometry. No inhibition in IFN-α production by monocytes was observed after cross-linking any of these cell surface receptors (data not shown).

Cross-linking cell surface receptors does not inhibit endocytosis in PDC

One possibility to explain the inhibition of IFN-α production following receptor cross-linking was that the binding of Abs and microbeads to the surface of the PDC was inhibiting the cell from coming in contact with or taking up virus. If this were the case, because the cell was not "seeing" the virus, IFN-α would not be produced. To study the endocytic ability of the PDC after cross-linking, we used the soluble fluorescent reagent, FITC-conjugated dextran. FITC-dextran is taken up by receptor-mediated endocytosis via the mannose receptor in MDDCs (31). Our laboratory has shown that the mannose receptor is expressed at low levels on PDC and this receptor is involved in the PDC IFN response to HSV, because blocking this receptor with mAb, mannan or certain monosaccharides leads to decreased IFN-α production (32). As shown in Fig. 3*A*, PDC were able to take up FITC-dextran in a time- and temperature-dependent manner, albeit to a lower extent than MDDCs. To determine whether cross-linking was having an affect on the endocytic ability of PDC, PBMC were cross-linked and incubated with FITC-dextran for 60 min at 37°C. As a negative control, PBMC were incubated with FITC-dextran on ice for 60 min to prevent uptake of the FITC-dextran. Cells were surface stained with CD123 PE and HLA-DR allophycocyanin or BDCA-2 PE and BDCA-4 allophycocyanin to gate on PDC. Fig. 3*B* shows that cross-linking BDCA-2, CD4, BDCA-4, or CD123 did not inhibit the ability of PDC to endocytose FITC-dextran as measured both by the percent of PDC taking up FITC-dextran and by the mean fluorescence intensity (MFI) of PDC that took up FITC-dextran. These results suggest that PDC are still capable of taking up Ag after cross-linking.

Cross-linking cell surface receptors does not induce apoptosis in PDC

Another possible mechanism by which cross-linking inhibits IFN-α production is through the induction of apoptosis in the cross-linked cells. It has been reported that cross-linking CD4 on T cells with soluble HIV gp120 causes apoptosis of these uninfected cells and enhances the ability of this virus to destroy $CD4^+$ T cells (33). More recently, cross-linking HLA-DR on CD40L-matured PDC, but not freshly isolated cells, was reported to induce apoptosis (34). To investigate whether a similar mechanism was at work here, we used annexin V staining. PBMC were cross-linked and incubated at 37°C for 6 h, then stained with Annexin V FITC and 7-AAD (the latter to detect necrotic cells), as well as CD123 PE and HLA-DR allophycocyanin or BDCA-2 PE and BDCA-4 allophycocyanin to stain PDC. As shown in Fig. 4*A*, following 6 h of incubation at 37°C, there was no significant difference in the annexin V staining of the non-cross-linked PDC compared with those cross-linked with either BDCA-2, BDCA-4, CD4, or CD123. We also looked at the activation of caspase-3 to determine whether apoptosis was occurring. Caspase-3 is a protease that is activated by cleavage during the early stages of apoptosis (35). After cross-linking, PBMC were incubated for 6 h at 37°C followed by surface staining for PDC-specific markers. Intracellular flow cytometry was performed using an Ab specific for activated caspase-3. The results show that there is no increase in activated caspase-3 after cross-linking any of the cell surface markers (Fig. 4*B*). Taken together, these results show that the decrease in IFN-α production after cross-linking is not due to apoptosis of PDC.

Cross-linking CD123 leads to PDC maturation

Another possible explanation for the observed effect of cross-linking on IFN-α production in PDC is induction of maturation. As PDC mature, they up-regulate MHC and costimulatory molecules, becoming potent APCs, while losing their ability to produce IFN-α (5, 7). To determine whether the PDC were maturing in response to cross-linking, PBMC were cross-linked and incubated for 18 h at 37°C. The cells were then surface stained for the expression of the costimulatory molecules CD80 and CD86, along with the PDC-specific stains CD123 PE and HLA-DR allophycocyanin or BDCA-2 PE and BDCA-4 allophycocyanin. CD123 cross-linking

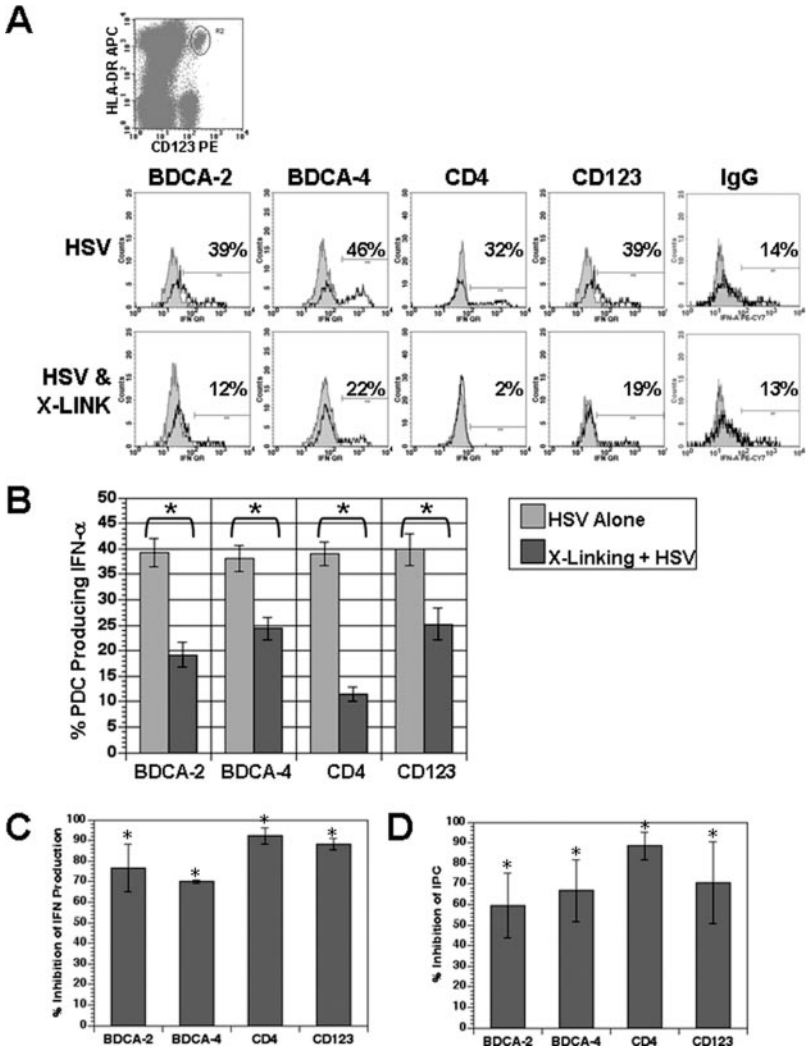

FIGURE 2. Cross-linking cell surface receptors on PDC with Ab and microbeads leads to the inhibition of IFN-α production and a decrease in IFN-α-producing cells in response to HSV. PMBC were incubated with Ab followed by anti-IgG1 microbeads or specific Ab-conjugated microbeads to cross-link BDCA-2, BDCA-4, CD4, or CD123 and stimulated with HSV-1 (MOI = 1) for 6 h. Mouse IgG isotype control Ab was used as a negative control. *A*, PBMC were surfaced stained with either CD123 PE and HLA-DR allophycocyanin (for BDCA-2, BDCA-4, CD4 cross-linking, *left panel*) or BDCA-2 PE and BDCA-4 allophycocyanin (for CD123 cross-linking) to gate on PDC, followed by intracellular staining for IFN-α production. Histogram overlays compare unstimulated PDC (gray filled histograms) with HSV-stimulated PDC (black line). *Top panels*, HSV stimulation without cross-linking; *bottom panels*, cells that have had their indicated cell surface receptor cross-linked prior to HSV stimulation. Percentages within each histogram denote the percentage of PDC-producing IFN-α after HSV stimulation. One representative experiment of 16–24 for each receptor cross-linked is shown. *B*, The mean percentage of PDC $\pm$ SEM (n = 16–24) producing IFN-α after HSV-1 stimulation alone (light gray bars) or cross-linking prior to HSV-1 stimulation (dark gray bars) is shown. $*$, Significant differences between HSV stimulation alone and cross-linking prior to HSV stimulation for each receptor cross-linked; p values of < 0.05 are considered significant. *C*, IFN-α production was measured by bioassay. Results show the percent inhibition of IFN-α production, with cells that were not cross-linked, having 0% inhibition. The mean percent inhibition $\pm$ SEM of $n = 3$ independent experiments is shown. $*$, Significant differences ($p < 0.05$) between no cross-linking and cross-linked cells. *D*, Frequency of IFN-α-producing cells was measured by ELISPOT assay. Results are shown as percent inhibition of IFN-α-producing cells, with the non-cross-linked cells having 0% inhibition. The mean percent inhibition $\pm$ SEM of $n = 3$ independent experiments is shown. $*$, Significant differences ($p < 0.05$) between no cross-linking and cross-linked cells.

induced the up-regulation of CD80 and CD86 (Fig. 5*A*). The expression levels of these molecules were comparable, and in the case of CD86, higher than that of PDC stimulated with HSV to induce maturation. We also looked at the cell surface expression of CD62L. CD62L is an L-selectin that allows PDC to migrate from the blood to lymph nodes through high endothelial venules. CD62L has been shown to be down-regulated on PDC as they mature (7). Indeed, in Fig. 5*B* we show that stimulating PDC with either IL-3 or IL-3 and TNF-α leads to the down-regulation of CD62L. Cross-linking of CD123 also induced the down-regulation of CD62L after 6 h incubation at 37°C (Fig. 5*B*, *third panel*). In contrast to the results of CD123, cross-linking of BDCA-2, BDCA-4, and CD4 did not induce any changes in the expression levels of CD80, CD86 (Fig. 5*A*), or CD62L (data not shown). These results suggest that cross-linking CD123 on the surface of PDC induces maturation leading to the down-regulation of IFN-α production, and this mechanism may be distinct from the down-regulation observed with cross-linking of the other cell surface markers.

Cross-linking BDCA-2 and BDCA-4, but not CD4, on PDC leads to an increase in tyrosine phosphorylation

It has been reported that BDCA-2 ligation induces *src*-family protein tyrosine kinase-dependent intracellular calcium mobilization

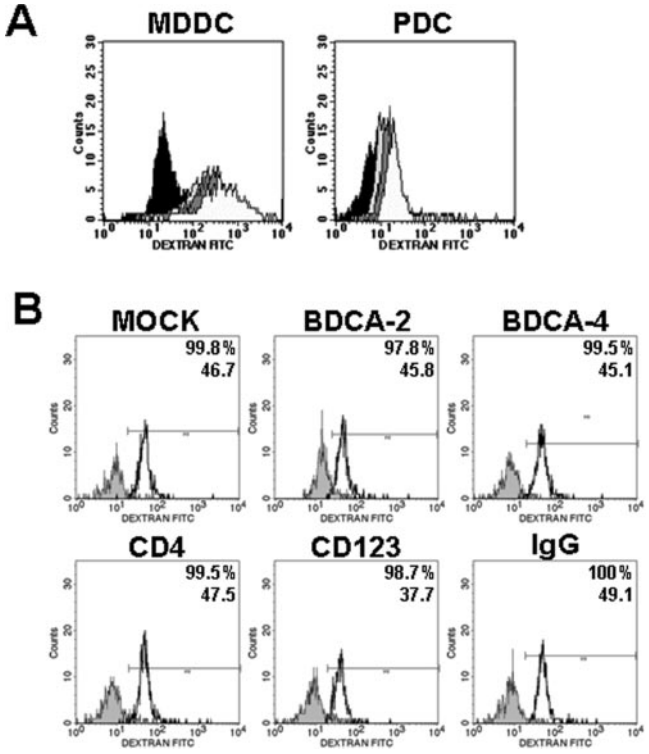

FIGURE 3. PDC take up FITC-dextran in a time- and temperature-dependent manner and independent of cell surface receptor cross-linking. *A*, MDDC and PBMC (1×10^6 cells) were incubated with FITC-dextran (1 mg/ml final concentration) at 0°C for 60 min (black histogram) or at 37°C for 15 (light gray histogram), 30 (dark gray histogram), or 60 (white histogram) min. PBMC were surfaced stained with CD123 PE and HLA-DR allophycocyanin to gate on PDC. One representative experiment of five is shown. *B*, BDCA-2, BDCA-4, CD4, and CD123 were cross-linked on PBMC with Ab followed by anti-IgG microbeads or Ab-conjugated microbeads. Mouse IgG isotype control Ab was used as a negative control. Cells were incubated with FITC-dextran for 60 min and surface stained with CD123 PE and HLA-DR allophycocyanin (for BDCA-2, BDCA-4, CD4 cross-linking) or BDCA-2 PE and BDCA-4 allophycocyanin (for CD123 cross-linking) to gate on PDC. Histogram overlays compare FITC-dextran uptake at 0°C (gray shaded histograms) and uptake at 37°C (black line). Numbers in the *upper right hand corner* of each histogram represent the percentage of PDC that took up FITC-dextran (*top*) and the MFI of the PDC that took up FITC-dextran (*bottom*). One representative experiment of five is shown for each cell surface receptor cross-linked.

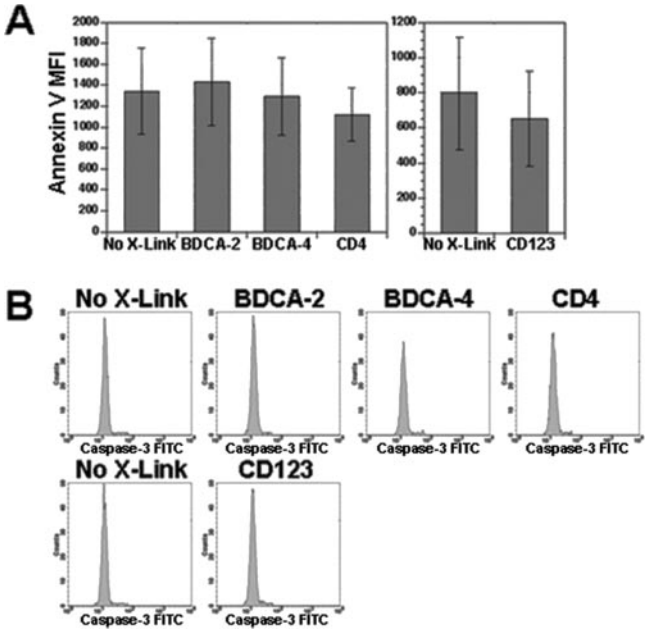

FIGURE 4. Cross-linking cell surface receptors on PDC does not induce apoptosis. BDCA-2, BDCA-4, CD4, and CD123 were cross-linked on PBMC as described in *Materials and Methods*. PBMC (2×10^6 cells/ml) were incubated at 37°C for 6 h. As a positive control for apoptosis, PBMC were heated to 56°C for 10 minutes (data not shown). *A*, After incubation, cells were stained with Annexin V FITC and 7-AAD, along with CD123 PE and HLA-DR allophycocyanin (BDCA-2, BDCA-4, CD4 cross-linking) or BDCA-2 PE and BDCA-4 allophycocyanin (CD123 cross-linking) staining to gate on PDC. The mean MFI of annexin V ± SEM of $n = 4$ experiments is shown. No significant difference in annexin V staining between cross-linked and non-cross-linked cells was detected. *B*, PBMC were surface stained with CD123 PE, HLA-DR PerCP, and CD11c allophycocyanin (for BDCA-2, BDCA-4, CD4 cross-linking) or BDCA-2 PE and BDCA-4 allophycocyanin (for CD123 cross-linking) to gate on PDC, followed by intracellular staining for activated caspase-3. One of five representative experiments is shown.

and protein tyrosine phosphorylation of intracellular proteins (19). To further investigate the role of signaling in the cross-linking of BDCA-2, BDCA-4, and CD4, we used anti-phosphotyrosine Ab in intracellular flow cytometry to determine the effect of cross-linking these receptors on tyrosine phosphorylation. PBMC were cross-linked and incubated for 0, 5, 10, 15, 30, and 60 min at 37°C. After incubation, the cells were immediately put on ice, then fixed with 1% paraformaldehyde and stored at 4°C overnight. The following day, the samples were surface stained for the PDC markers CD123 and HLA-DR, followed by intracellular staining using an anti-phosphotyrosine Ab. BDCA-2 cross-linking led to an increase in phosphorylated tyrosine that could be seen at 5 min, but returned to control levels by 10 min (Fig. 6). BDCA-4 cross-linking led to an increase in phosphorylated tyrosine after 10 min that again returned to control levels within 5 min. However, after CD4 cross-linking, no change in the levels of phosphorylated tyrosine was observed in the first 15 min (Fig. 6, *bottom*) and even up to 60 min (data not shown). These results suggest that cross-linking BDCA-2 and BDCA-4 induces a signaling cascade indicated by tyrosine phosphorylation, whereas CD4 cross-linking may be operating by a different mechanism or different kinetics. Due to technical difficulties involving PDC surface staining, this experiment could not be performed on CD123 cross-linked cells. To gate on PDC after CD123 cross-linking, either BDCA-2 or BDCA-4 Ab must be used. However, this experimental protocol calls for fixing the cells before staining the surface for PDC-specific markers. Under these conditions, we could not detect BDCA-2- or BDCA-4-positive PDC, most likely because fixation is changing the conformation of the BDCA-4 and BDCA-2 receptors preventing these Abs from binding to the appropriate epitope (36).

Cross-linking cell surface receptors on PDC does not affect constitutive or induced levels of IRF-7

The IRF family of transcription factors is important in the regulation of IFN-α production with IRF-3, -5, and -7 all implicated in IFN-α production (37, 38). In PDC, IRF-7 is expressed at high constitutive levels and is further up-regulated in response to HSV and IFN-α stimulation (26, 29, 39) (Fig. 7*A*). We postulate that these high constitutive levels of IRF-7 may be what allow PDC to be such potent producers of IFN-α as compared with other cells. Therefore, to investigate what role cross-linking might have on levels of IRF-7 expression, PBMC were cross-linked, then either mock, HSV, or IFN-α stimulated, and incubated for 6 h at 37°C. Intracellular flow cytometry for IRF-7 was performed. The results

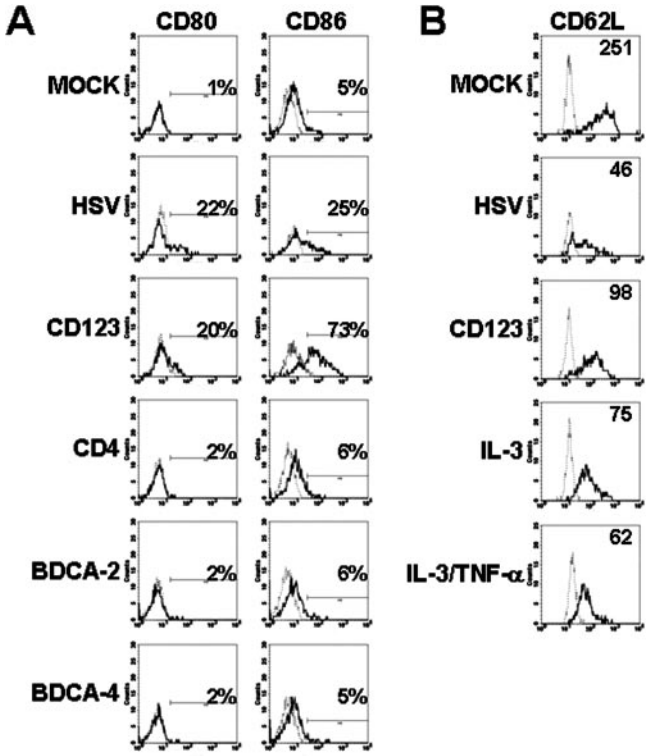

FIGURE 5. Cross-linking CD123, but not BDCA-2, BDCA-4, or CD4 on PDC induces the up-regulation of CD80 and CD86 and the down-regulation of CD62L. BDCA-2, BDCA-4, CD4, and CD123 were cross-linked on PBMC as described in *Materials and Methods*. *A*, PBMC (2×10^6 cells/ml) were stimulated with HSV-1 (MOI = 1) for 18 h. PMBC were surface stained with CD123 PE, HLA-DR PerCP, and CD11c allophycocyanin (for BDCA-2, BDCA-4, CD4 cross-linking) or BDCA-4 PE, HLA-DR PerCP, and CD11c allophycocyanin (for CD123 cross-linking) to gate on PDC, along with CD80 FITC or CD86 FITC. Histogram overlays show IgG1 isotype control (dashed line) and CD80 (*left column*) or CD86 (*right column*) expression (black line). The percentage of PDC positive for CD80 or CD86 is shown in the *upper right corner* of each histogram. One representative experiment of four to six is shown. *B*, CD123 was cross-linked on PBMC (2×10^6 cells/ml) as described and cells were incubated for 6 h. Alternatively, PBMC were stimulated with HSV-1 (MOI = 1), IL-3 (100 IU/ml), or IL-3 and TNF-α (100 IU/ml) for 6 h. Cells were surface stained with or BDCA-2 PE and BDCA-4 allophycocyanin to gate on PDC, along with CD62L FITC. Histogram overlays show IgG2a isotype control (dashed line) and CD62L expression (black line). The MFI for CD62L is shown in the *upper right corner* of each histogram. One representative experiment of three is shown.

show that cross-linking had no effect on IRF-7 levels with or without stimulation (Fig. 7*B*). PDC that had their receptors cross-linked were still able to up-regulate IRF-7 in response to HSV and IFN-α to the same extent as non-cross-linked cells.

Cross-linking BDCA-2, BDCA-4, and CD4, but not CD123, on PDC inhibits the nuclear translocation of IRF-7

Upon stimulation with HSV, IRF-7 is up-regulated in the cytoplasm and translocated to the nucleus were it acts as a transcription factor for the *IFN-α* genes. In PDC, IRF-7 is translocated to the nucleus within 2 h of stimulation with HSV, as shown by fluorescence microscopy (29). Preliminary experiments using this technique showed that cross-linking CD4 on PDC inhibited the nuclear translocation of IRF-7 in response to stimulation with HSV (data not shown). However, only low numbers of PDC (10–20 cells/sample) could be visualized from each sample under the microscope, making statistical analysis difficult.

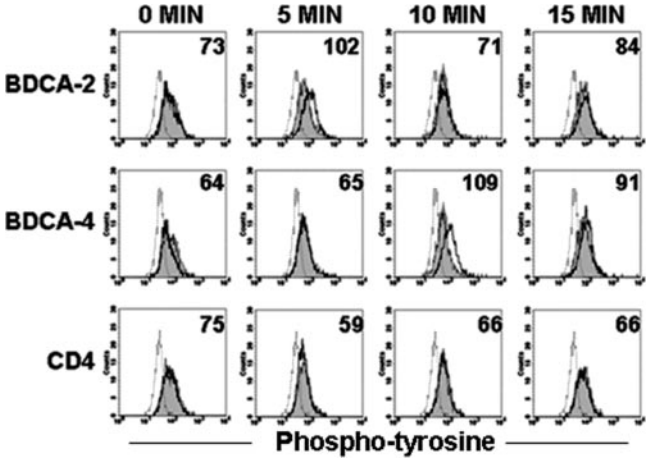

FIGURE 6. Cross-linking BDCA-2 and BDCA-4, but not CD4, on PDC induces tyrosine phosphorylation. BDCA-2, BDCA-4, and CD4 were cross-linked on PBMC on ice. PBMC were incubated at 37°C for the time points indicated, immediately put on ice, and fixed with 1% paraformaldehyde in PBS. The following day, cells were surface stained with CD123 PE and HLA-DR allophycocyanin, followed by intracellular staining for phosphorylated tyrosine. Histogram overlays show IgG2b isotype control (dashed line), PDC incubated at 0°C (gray histogram), and PDC incubated at 37°C (black line). The MFI of phosphotyrosine staining in PDC incubated at 37°C is shown. One representative experiment of three is shown.

To more quantitatively determine whether cross-linking cell surface receptors was inhibiting the translocation of IRF-7, we used a new technology developed by the Amnis Corporation, the ImageStream, which combines high resolution digital imaging with flow cytometry. PDC were enriched from PBMC by negative selection

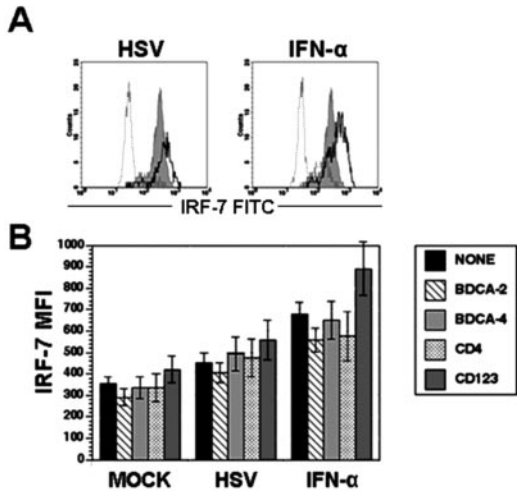

FIGURE 7. Cross-linking cell surface receptors on PDC does not have an effect on HSV and IFN-α-induced levels of IRF-7. BDCA-2, BDCA-4, CD4, and CD123 were cross-linked on PBMC as described in *Materials and Methods*. PBMC (2×10^6 cells/ml) were stimulated with HSV-1 (MOI = 1) or recombinant human IFN-α2b (10,000 IU) for 6 h. PBMC were surface stained with CD123 PE and HLA-DR allophycocyanin (BDCA-2, BDCA-4, CD4) or BDCA-2 PE and BDCA-4 allophycocyanin (CD123) to gate on PDC, followed by intracellular staining for IRF-7. *A*, Histogram overlays show rabbit Ig isotype control (dashed line) and IRF-7 expression in unstimulated PDC (gray histogram) and HSV (*left panel*, black line) or IFN-α (*right panel*, black line) stimulated PDC. *B*, The mean MFI of IRF-7 ± SEM of $n = 6$–10 experiments is shown. No significant difference between cross-linked and non-cross-linked cells was found for any of the conditions tested.

and cell surface receptors were cross-linked as described above. Cells were stimulated with HSV-1 (MOI = 1) for 3 h followed by surface staining for BDCA-2 and BDCA-4 and intracellular staining for IRF-7. Immediately before acquisition, nuclei were stained with 7-AAD. Images were captured in five channels: darkfield, brightfield, Alexa Fluor 488, PE, and 7-AAD and images were analyzed using IDEAS software as described in *Materials and Methods* and in George et al. (27). Single BDCA-2/4-positive IRF-7^{bright} cells were identified as PDC as shown in the gates in Fig. 8, *A* and *B*. Fig. 8*C* shows the quantitation of nuclear translocation of IRF-7 using histograms of the IRF-7/7-AAD similarity scores. Stimulation of PDC with HSV increased the percentage of PDC with nuclear-localized IRF-7 (9.6% vs 3.2% of mock). Cross-linking BDCA-2, BDCA-4, and CD4 before HSV stimulation inhibited the translocation of IRF-7 as measured by the decreased percentage of cells with nuclear-localized IRF-7 compared with HSV-stimulated, non-cross-linked cells (anti-BDCA-2: 2.7%; anti-BDCA-4: 2.9%; anti-CD4: 1.4%) in a statistically significant manner (Fig. 8*C*). Interestingly, CD123 cross-linking did not inhibit IRF-7 translocation (10.0%), giving further evidence that cross-linking this receptor inhibits IFN-α production by a different mechanism than cross-linking other receptors. Representative images of PDC determined to have untranslocated, cytoplasmic IRF-7 or translocated, nuclear IRF-7 are shown in Fig. 8, *D* and *E*, respectively.

Discussion

The regulation of IFN-α production by PDC is not well-understood, but is important in understanding how these cells contribute to the immune response to viral pathogens. The discovery that cross-linking cell surface receptors on PDC has an effect on their ability to produce IFN-α may lead to the elucidation of a pathway by which IFN-α is regulated in these cells. In fact, the effect of receptor cross-linking on the regulation of immune responses has been well-documented in a variety of cell types. For instance, it has been reported that cross-linking of MHC class I molecules on NK cells induces intracellular phosphotyrosines and inhibits NK cell function (40). Cross-linking MHC class II on MDDC has been

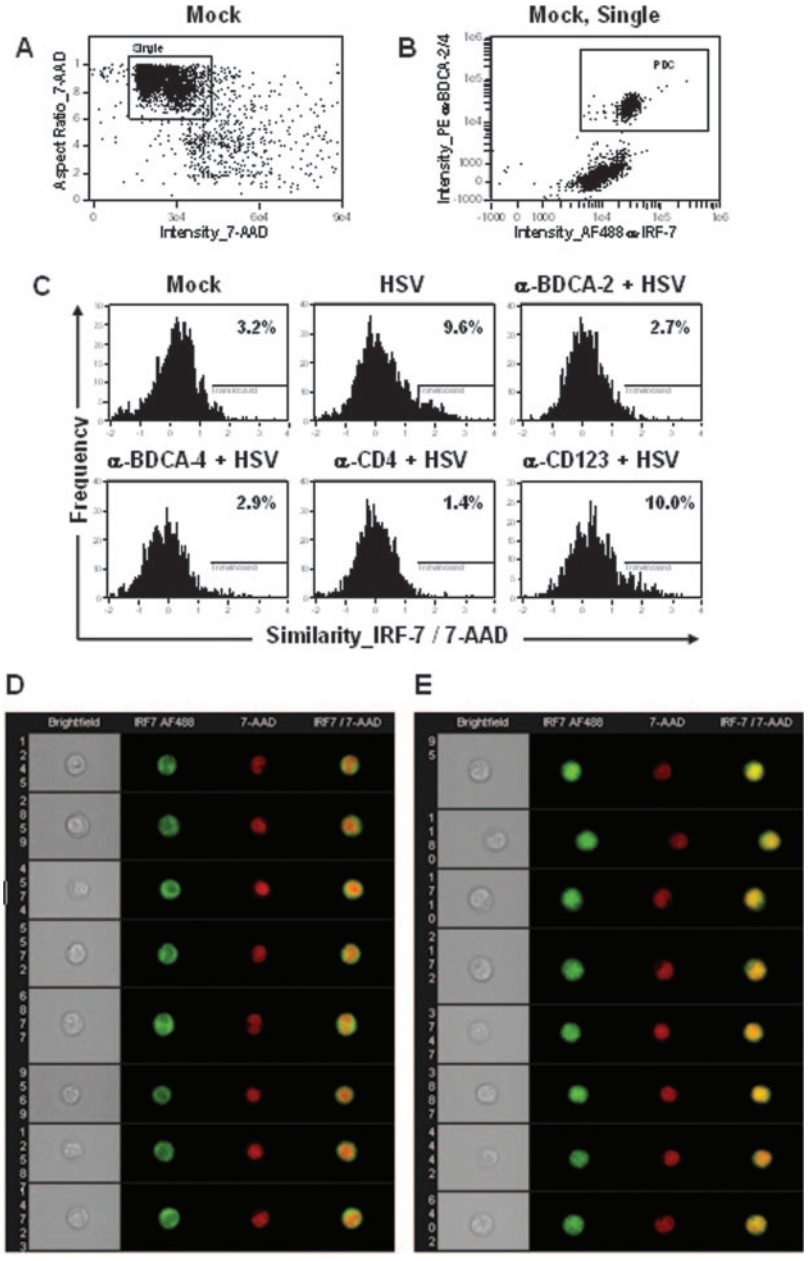

FIGURE 8. Cross-linking BDCA-2, BDCA-4, and CD4, but not CD123, inhibits nuclear translocation of IRF-7. BDCA-2, BDCA-4, CD4, and CD123 were cross-linked on PDC followed by stimulation with HSV-1 (MOI = 1) for 3 h at 37°C. Following stimulation, cells were probed as described for IRF-7, BDCA-2, and BDCA-4 expression and for nuclear morphology with 7-AAD, then run on the ImageStream. Image data was then analyzed to determine the percentage of PDC with nuclear-localized IRF-7. Single cells were identified as 7-AAD-positive events with high nuclear aspect ratios (*A*), followed by gating on the BDCA2/4^{+} IRF-7^{bright} population to identify PDC (*B*). The correlation between the pixel intensities of the IRF-7 and 7-AAD images (the similarity_IRF-7/7-AAD score) of single PDC is plotted in the histograms (*C*). Cells with nuclear localized IRF-7 have high values because the appearance of the IRF-7 and 7-AAD images are similar, while cells with cytoplasmic IRF-7 distributions have low values because the images appear as opposites. The numbers in the *upper right corner* of each histogram show the percentage of cells with nuclear-localized IRF-7. Representative images of PDC from the mock treatment group that fall to the left of the "Translocated" region are shown in *D* and PDC from the HSV treatment group that fall within the "Translocated" region are shown in *E*. One experiment representative of three similar experiments is shown.

shown to induce maturation, while cross-linking on matured MDDC led to the induction of apoptosis of these cells (41). Chieppa et al. (42) have reported that cross-linking of the mannose receptor on MDDC induces the production of anti-inflammatory cytokines and produces chemokines that direct Th2 and regulatory T cells and negatively regulate Th1 polarization. It has also been reported that MDDC derived from monocytes isolated by positive selection via anti-CD14 microbeads had a reduced capacity to produce IL-12, IL-10, and TNF-α in response to LPS stimulation as compared with MDDC generated from monocytes isolated by plastic adherence (43). In the case of PDC, cross-linking HLA-DR on CD40L-matured PDC, but not freshly isolated cells, has been shown to induce apoptosis of these cells (34). Dzionek et al. (19) have reported that ligation with BDCA-2 Ab causes intracellular calcium mobilization and protein-tyrosine phosphorylation leading to an inhibition of IFN-α production in response to influenza virus, anti-dsDNA mAb, and unmethylated plasmid DNA, sera from systemic lupus erythematosus (SLE) patients, and CpG oligonucleotides. They therefore postulate that BDCA-2 plays a role in the regulation of IFN-α production. Similar results were obtained by Blomberg et al. (44), who studied the role of BDCA-2 and BDCA-4 on IFN-α production by PDC in patients with SLE. They found that while BDCA-2 mAb inhibited IFN-α production in response to SLE-IFN-α-inducing factor (IIF) (SLE serum containing endogenous IIF) and HSV-1 in both SLE patients and healthy controls, BDCA-4 mAb only partially inhibited SLE-IIF-induced IFN-α production and failed to inhibit IFN-α production in HSV-1-stimulated cells. Other studies performed by Kerkmann et al. (24) have shown that BDCA-2 Ab ligation inhibits CpG-induced IFN-α, IFN-β, and TNF-α synthesis. They too looked at intracellular calcium fluxes after Ab ligation and found that BDCA-2, but not BDCA-4, Ab ligation led to an increase in intracellular calcium. They found that the mechanism by which BDCA-2 interacts with the IFN-α pathway is distinct and independent of the IFNR-mediated feedback loop in which the IFN-α made by the cell binds to the IFNR in an autocrine fashion leading to the production of more IFN-α.

In the present study, we show that rather than being limited to BDCA-2 cross-linking, cross-linking a wide variety of cell surface receptors on PDC leads to the inhibition of IFN-α production in response to stimulation with HSV-1. In some cases, this phenomenon may not be dependent on a secondary cross-linking agent (in this case magnetic immunobeads) and can be observed with Ab ligation alone. For example, BDCA-2 Ab alone caused an inhibition in IFN-α production, which was enhanced by cross-linking with a secondary Ab or microbead. In contrast, CD4 Ab alone did not have an effect on IFN-α production; the CD4 must be cross-linked with microbeads or secondary Ab to observe the impairment. Dzionek et al. (20) have reported that cross-linking CD54, CD58, and CD62L on PDC has no effect on IFN-α production, however, these receptors were cross-linked with Ab alone. As we have shown, some receptors, including CD62L, require secondary cross-linking to get significant IFN-α inhibition. We have not found any cell surface receptor that does not impair IFN-α production when cross-linked with secondary Ab or Ab-conjugated microbeads.

We investigated several possibilities to explain this cross-linking phenomenon. To begin with, cross-linking may inhibit the virus from coming in contact with or being endocytosed by the PDC. We used FITC-conjugated dextran to examine the endocytic ability of PDC after cell surface cross-linking. Although it has been reported that PDC are not very endocytic (5), we demonstrated that PDC do take up FITC-conjugated dextran, albeit to a lower extent than monocyte-derived DCs. The results show that PDC are still capable of taking up FITC-dextran after cross-linking cell surface receptors. It has also been shown by Dzionek et al. (20) that cross-linking BDCA-2 1 h after stimulating with influenza virus still leads to the inhibition in IFN-α production. Taken together, these results suggest cross-linking cell surface receptors on PDC does not affect endocytosis.

To investigate the possibility that cross-linking was inducing PDC apoptosis, we used annexin V staining, as well as intracellular staining for activated caspase-3. There was no increase in annexin V binding or activated caspase-3 in cells that were cross-linked as compared with those that were left untouched. The results indicate that cell surface receptor cross-linking on PDC is not inducing apoptosis and another mechanism is responsible for the decrease in IFN-α production. This leads us to the next hypothesis, PDC maturation. It is known that as PDC mature, they up-regulate costimulatory molecules and lose their ability to produce IFN-α (5, 7, 45). To investigate this possibility, we looked at the up-regulation of costimulatory molecules, CD80 and CD86, on PDC after cell surface cross-linking. The results showed that CD123, but not BDCA-2, BDCA-4, or CD4 cross-linking induces the up-regulation of CD80 and CD86 on PDC. We also looked at the expression of CD62L, which is highly expressed on immature PDC and is down-regulated as they mature (7). Cross-linking CD123, but not BDCA-2, BDCA-4, or CD4, led to the down-regulation of CD62L on PDC. This suggests that CD123 cross-linking is impairing IFN-α production by inducing PDC maturation. CD123 is the IL-3R and it is known that IL-3 is a survival factor for PDC and induces their maturation (5). Therefore, cross-linking the IL-3R appears to be acting in an agonistic manner, inducing PDC maturation. Although IL-3 alone is not known to inhibit IFN-α production in PDC in vitro, it is possible that cross-linking CD123 induces multiple signaling pathways, one that induces up-regulation of costimulatory molecules, and one that leads to the inhibition of IFN-α. It is also possible that the cross-linking of CD123 is a stronger stimulus than IL-3 itself; therefore, the cells are maturing faster and are rapidly losing their ability to make IFN-α.

It has been reported that ligation of BDCA-2 leads to calcium mobilization and protein tyrosine phosphorylation indicating the induction of a signaling pathway that may negatively regulate IFN-α production (19). We performed intracellular flow cytometry for phosphorylated tyrosine to determine whether a similar event is occurring when other cell surface receptors are cross-linked. The results show that BDCA-2 and BDCA-4 cross-linking induce tyrosine phosphorylation. This event is rapid and transient, occurring within the first 5–10 min after cross-linking and returning to control levels within 5 min. Interestingly, no increase in tyrosine phosphorylation was observed after CD4 cross-linking. These results suggest that BDCA-2 and BDCA-4 are activating a signaling pathway, while a different mechanism may be at work after CD4 cross-linking. It is also possible that the kinetics of CD4 cross-linking differ from that of BDCA-2 and BDCA-4. For example, cross-linking CD4 may cause transient tyrosine phosphorylation at a rate too fast for us to measure.

The IFN regulatory factors play a pivotal role in the IFN-α induction pathway. In most cell types, IRF-3 is expressed constitutively. Upon viral stimulation, IRF-3 is phosphorylated and translocates to the nucleus where it acts as a transcription factor for the *IFN-β* gene and some *IFN-α* genes. This IFN works in an autocrine fashion to induce the translation of IRF-7. This newly synthesized IRF-7 can then be phosphorylated and form homodimers or heterodimers with IRF-3, translocate to the nucleus and act as a transcription factor for all the *IFN-α* genes (37, 46). The role of IRFs in regulating IFN-α production has been elucidated in fibroblasts, but how these transcription factors work in

PDC is still under investigation. It is known that IRF-7 is constitutively expressed at very high levels in PDC and that its expression is further up-regulated by HSV and IFN-α stimulation. We postulate that these high levels of constitutive IRF-7 allow for the rapid expression of large quantities of IFN-α by PDC without the need for the aforementioned autocrine feedback loop. As in other cells, after viral stimulation, IRF-7 is phosphorylated, forms homodimers, and is translocated from the cytoplasm to the nucleus where it acts as a transcription factor for *IFN-α* genes (26, 29, 39). Because IRF-7 plays a large part in the production of IFN-α, it may also play a pivotal role in the regulation of this cytokine. To explore how cross-linking may impact IRF-7, we used intracellular flow cytometry and fluorescent microscopy to measure the levels of cytoplasmic IRF-7 and IRF-7 nuclear translocation, respectively. The results show that cross-linking CD4, BDCA-2, BDCA-4, or CD123 does not affect constitutive levels of IRF-7 and furthermore, does not inhibit HSV and IFN-α-induced up-regulation of IRF-7. However, using fluorescent microscopy, results suggest that CD4 cross-linking inhibits HSV-induced IRF-7 nuclear translocation.

Although we have been successful in demonstrating nuclear translocation using fluorescent microscopy, this technique is not optimal. Nuclear translocation as determined by eye is very subjective and cannot be thoroughly quantitated. In addition, only a limited number of cells can be viewed using this method. To more comprehensively investigate the effect of cross-linking on IRF-7 nuclear translocation, we used the ImageStream imaging flow cytometer. This machine is a flow cytometer that captures up to six multispectral digital images of each cell. This technology allowed us to collect several hundred PDC images and objectively score IRF-7 translocation using image similarity analysis. Using the ImageStream, we show that cross-linking BDCA-2, BDCA-4, and CD4 inhibits IRF-7 nuclear translocation in a statistically significant manner, while cross-linking CD123 does not. It is not surprising that CD123 cross-linking behaved differently than cross-linking other receptors, as this was shown to induce PDC maturation, while others did not. This is further evidence that CD123 cross-linking works by a different mechanism to inhibit IFN-α production. Because PDC that had CD123 cross-linked were still able to translocate IRF-7, IFN-α may be regulated post-transcriptionally, possibly at the level of mRNA stability. Alternatively, the ability of IRF-7 to bind to DNA after nuclear translocation and act as a transcription factor may be affected. It is known that acetylation of the DNA-binding domain of IRF-7 inhibits its ability to bind DNA (47). It is also possible that while cross-linking CD123 does not affect IRF-7 in PDC, it might have an impact on another IRF important for IFN-α production. Although IRF-7 is indeed an important player in the regulation of IFN-α production, it is not the only one. IRF-3, and more recently, IRF-5, have also been shown to play a part in this pathway. Both are constitutively expressed by PDC and it is believed that different IRFs are induced by different viruses and lead to the production of distinct subsets of *IFN-α* genes (38, 48).

Investigating this cross-linking phenomenon leads to the question, what is the in vivo correlate of cross-linking with Ab-conjugated microbeads? The answer may lie in the role that BDCA-2, BDCA-4, and CD4 play in PDC function. Although it has recently come to light that BDCA-2 acts as an endocytic receptor on PDC, its ligands have yet to be determined (19). Given its endocytic nature, it would seem unlikely that the natural ligands for this receptor would solely serve to turn off the PDC. It is possible that the BDCA-2 Ab binds to a different epitope on the receptor than the natural ligand, leading to different outcomes. BDCA-4 has been recently identified as NP-1, a neuronal receptor for the axon guidance factors belonging to the class-3 semaphorin subfamily. It is also expressed by endothelial and tumor cells as a receptor for VEGF-A and plays a major role in angiogenesis (20). The effects of VEGF-A on PDC have not been reported and experiments are currently underway in our laboratory to investigate its impact on IFN-α production by these cells. Tordjman et al. (21) have shown the expression of NP-1 on MDDC and resting T cells and have suggested a role for NP-1 in the initiation of the primary immune response. Although it is well-known how CD4 interacts on a T cell to assist in T cell-APC interaction, its role on PDC has yet to be explained. It is possible that when a PDC interacts with a naive T cell, the CD4 molecules on each cell interact within the immunological synapse. In doing so, the T cell may signal the PDC through CD4 to shut off IFN-α production. Another possibility is that this molecule may be involved in DC:DC communication through a CD4:HLA-DR interaction. Because the natural ligands for these receptors are still unknown, it is yet to be determined whether the binding of the natural ligand to the receptor will result in similar outcome to receptor cross-linking with Ab. It is possible that in vitro cross-linking of cell surface receptors leads to overstimulation of the cell, which induces a pathway to shut off the cell instead of activating it like a natural ligand might do. Deciphering the in vivo function of these receptors on PDC will help determine their role in regulating IFN-α production.

The results of this study should be taken into consideration when investigating PDC. Many investigators use BDCA-4 cell isolation kits to enrich PDC from PBMC. We have shown that cross-linking BDCA-4 on PDC leads to decreased IFN-α production in response to viral stimulation and it is still unknown what other effects positive selection might have on these cells. Therefore, investigators must keep this in mind when using this technique to purify PDC. Positive selection may not be appropriate method to purify these cells when studying them in a functional assay. When highly purified PDC are required, our laboratory has used a technique in which PDC are first enriched from PBMC by negative selection. These enriched PDC can be stimulated, followed by positive selection to obtain highly purified PDC. This allows the stimulation to occur before positive selection without the need to stimulate large numbers of cells.

In conclusion, we have shown that the inhibition of IFN-α production after CD123 cross-linking is due to the stimulation of the IL-3R and induction of PDC maturation. It is likely that BDCA-2, BDCA-4, and CD4 cross-linking induce perhaps different signaling pathways that lead to regulation of IFN-α at the level of IRF-7. In the immune system, it is important to have mechanisms to turn off the immune response, for overactivation of immune cells or overproduction of immune products can lead to negative consequences. In the case of PDC, these cells make huge amounts of IFN-α. Although this is beneficial in the context of viral infection, production of this cytokine must be tightly regulated so that production is ceased when the infection is cleared or is not produced in the absence of infection. Elucidating the mechanism(s) by which IFN-α is regulated will help in understanding the role of PDC in the immune response and will help uncover how IFN-α may be used as a treatment in disease states or help control IFN-α production in diseases such as SLE, where overproduction of IFN-α contributes to disease pathogenesis.

Disclosures

The authors have no financial conflict of interest.

References

1. Megjugorac, N., H. Young, S. Amrute, S. Olshalsky, and P. Fitzgerald-Bocarsly. 2004. Virally stimulated plasmacytoid dendritic cells produce chemokines and induce migration of T and NK cells. *J. Leukocyte Biol.* 75: 504–514.

2. Penna, G., M. Vulcano, A. Roncari, F. Facchetti, S. Sozzani, and L. Adorini. 2002. Cutting edge: differential chemokine production by myeloid and plasmacytoid dendritic cells. *J. Immunol.* 169: 6673–6676.
3. Poeck, H., M. Wagner, J. Battiany, S. Rothenfusser, D. Wellisch, V. Hornung, B. Jahrsdorfer, T. Giese, S. Endres, and G. Hartmann. 2004. Plasmacytoid dendritic cells, antigen, and CpG-C license human B cells for plasma cell differentiation and immunoglobulin production in the absence of T-cell help. *Blood* 103: 3058–3064.
4. Jego, G., K. Palucka, J. P. Blanck, C. Chalouni, V. Pascual, and J. Banchereau. 2003. Plasmacytoid dendritic cells induce plasma cell differentiation through type I interferon and interleukin 6. *Immunity* 19: 225–234.
5. Grouard, G., M. Rissoan, L. Filguiera, I. Durand, J. Banchereau, and J. Liu. 1997. The enigmatic plasmacytoid T cells develop into dendritic cells with interleukin-3 and CD40 ligand. *J. Exp. Med.* 185: 1101–1111.
6. Kadowaki, N., S. Antonenko, J. Y. Lau, and Y. J. Liu. 2000. Natural interferon α/β-producing cells link innate and adaptive immunity. *J. Exp. Med.* 192: 219–226.
7. Cella, M., F. Facchetti, A. Lanzavecchia, and M. Colonna. 2000. Plasmacytoid dendritic cells activated by influenza virus and CD40L drive a potent TH1 polarization. *Nat. Immunol.* 1: 305–310.
8. Siegal, F., N. Kadowaki, M. Shodell, P. Fitzgerald-Bocarsly, K. Shah, S. Ho, A. Antonenko, and Y. J. Liu. 1999. The nature of the principal type 1 interferon-producing cells in human blood. *Science* 284: 1835–1837.
9. Feldman, S. B., M. Ferraro, H. M. Zheng, N. Patel, S. Gould-Fogerite, and P. Fitzgerald-Bocarsly. 1994. Viral induction of low frequency interferon-α producing cells. *Virology* 204: 1–7.
10. Svensson, H., B. Cederblad, M. Lindahl, and G. Alm. 1996. Stimulation of natural interferon-α/β-producing cells by *Staphylococcus aureus*. *J. Interferon Cytokine Res.* 16: 7–16.
11. Remoli, M. E., E. Giacomini, G. Lutfalla, E. Dondi, G. Orefici, A. Battistini, G. Uze, S. Pellegrini, and E. M. Coccia. 2002. Selective expression of type I IFN genes in human dendritic cells infected with *Mycobacterium tuberculosis*. *J. Immunol.* 169: 366–374.
12. Gibson, S. J., J. M. Lindh, T. R. Riter, R. M. Gleason, L. M. Rogers, A. E. Fuller, J. L. Oesterich, K. B. Gorden, X. Qui, S. W. McKane, et al. 2002. Plasmacytoid dendritic cells produce cytokines and mature in response to the TLR7 agonists, imiquimod and resiquimod. *Cell. Immunol.* 218: 74–86.
13. Kadowaki, N., S. Antonenko, and Y. J. Liu. 2001. Distinct CpG DNA and polyinosinic-polycytidylic acid double-stranded RNA, respectively, stimulate CD11c-type 2 dendritic cell precursors and $CD11c^+$ dendritic cells to produce type I IFN. *J. Immunol.* 166: 2291–2295.
14. Kadowaki, N., S. Ho, S. Antonenko, R. W. Malefyt, R. A. Kastelein, F. Bazan, and Y. J. Liu. 2001. Subsets of human dendritic cell precursors express different Toll-like receptors and respond to different microbial antigens. *J. Exp. Med.* 194: 863–869.
15. Krug, A., S. Rothenfusser, V. Hornung, B. Jahrsdorfer, S. Blackwell, Z. K. Ballas, S. Endres, A. M. Krieg, and G. Hartmann. 2001. Identification of CpG oligonucleotide sequences with high induction of IFN-α/β in plasmacytoid dendritic cells. *Eur. J. Immunol.* 31: 2154–2163.
16. Krug, A., A. Towarowski, S. Britsch, S. Rothenfusser, V. Hornung, R. Bals, T. Giese, H. Engelmann, S. Endres, A. M. Krieg, and G. Hartmann. 2001. Toll-like receptor expression reveals CpG DNA as a unique microbial stimulus for plasmacytoid dendritic cells which synergizes with CD40 ligand to induce high amounts of IL-12. *Eur. J. Immunol.* 31: 3026–3037.
17. Svensson, H., A. Johannisson, T. Nikkila, G. V. Alm, and B. Cederblad. 1996. The cell surface phenotype of human natural interferon-α producing cells as determined by flow cytometry. *Scand. J. Immunol.* 44: 164–172.
18. Dzionek, A., A. Fuchs, P. Schmidt, S. Cremer, M. Zysk, S. Miltenyi, D. W. Buck, and J. Schmitz. 2000. BDCA-2, BDCA-3, and BDCA-4: three markers for distinct subsets of dendritic cells in human peripheral blood. *J. Immunol.* 165: 6037–6046.
19. Dzionek, A., Y. Sohma, J. Nagafune, M. Cella, M. Colonna, F. Facchetti, G. Gunther, I. Johnston, A. Lanzavecchia, T. Nagasaka, et al. 2001. BDCA-2, a novel plasmacytoid dendritic cell-specific type II c-type lectin, mediates antigen capture and is a potent inhibitor of interferon α/β induction. *J. Exp. Med.* 194: 1823–1834.
20. Dzionek, A., Y. Inagaki, K. Okawa, J. Nagafune, J. Rock, Y. Sohma, G. Winkels, M. Zysk, Y. Yamaguchi, and J. Schmitz. 2002. Plasmacytoid dendritic cells: from specific surface markers to specific cellular functions. *Hum. Immunol.* 63: 1133–1148.
21. Tordjman, R., Y. Lepelletier, V. Lemarchandel, M. Cambot, P. Gaulard, O. Hermine, and P. H. Romeo. 2002. A neuronal receptor, neuropilin-1, is essential for the initiation of the primary immune response. *Nat. Immunol.* 3: 477–482.
22. Cederblad, B., and G. Alm. 1990. Infrequent but efficient interferon-α-producing human mononuclear leukocytes induced by herpes simplex virus in vitro studies by immunoplaque and limiting dilution assays. *J. Interferon Res.* 10: 65–73.
23. Howell, D., S. Feldman, P. Kloser, and P. Fitzgerald-Bocarsly. 1994. Decreased frequency of natural interferon producing cells in peripheral blood of patients with the acquired immune deficiency syndrome. *Clin. Immunol. Immunopath.* 71: 223–230.
24. Kerkmann, M., S. Rothenfusser, V. Hornung, A. Towarowski, M. Wagner, A. Sarris, T. Giese, S. Endres, and G. Hartmann. 2003. Activation with CpG-A and CpG-B oligonucleotides reveals two distinct regulatory pathways of type I IFN synthesis in human plasmacytoid dendritic cells. *J. Immunol.* 170: 4465–4474.
25. Fitzgerald, P. A., P. von Wussow, and C. Lopez. 1982. Role of interferon in natural kill of HSV-1 infected fibroblasts. *J. Immunol.* 129: 819–824.
26. Izaguirre, A., B. J. Barnes, S. Amrute, W.-S. Yeow, N. Megjugorac, J. Dai, D. Feng, E. Chung, P. M. Pitha, and P. Fitzgerald-Bocarsly. 2003. Comparative analysis of IRF and IFN-α expression in human plasmacytoid and monocyte-derived dendritic cells. *J. Leukocyte Biol.* 74: 1125–1138.
27. George, T., S. Fanning, P. Fitzgerald-Bocarsly, R. Medeiros, S. Highfill, Y. Shiizu, B. Hall, K. Frost, D. Basiji, W. Ortyn, et al. 2006. Quantitative measurement of nuclear translocation events using similarity analysis of multispectral cellular images obtained in flow. *J. Immunol. Methods* 311: 117–129.
28. Feldman, M., and P. Fitzgerald-Bocarsly. 1990. Sequential enrichment and immunocytochemical visualization of human interferon-α producing cells. *J. Interferon Res.* 10: 435–446.
29. Dai, J. H., N. Megjugorac, S. Amrute, and P. Fitzgerald-Bocarsly. 2004. Regulation of IRF-7 and IFN-α production by enveloped virus and LPS in human plasmacytoid dendritic cells. *J. Immunol.* 173: 1535–1548.
30. Olshalsky, S. L., and P. Fitzgerald-Bocarsly. 2005. Flow cytometric techniques for studying plasmacytoid dendritic cells in mixed populations. *Methods Mol. Med.* 116: 183–194.
31. Sallusto, F., M. Cella, C. Danieli, and A. Lanzavecchia. 1995. Dendritic cells use macropinocytosis and the mannose receptor to concentrate macromolecules in the major histocompatibility complex class II compartment: downregulation by cytokines and bacterial products. *J. Exp. Med.* 182: 389–400.
32. Milone, M. C., and P. Fitzgerald-Bocarsly. 1998. The mannose receptor mediates induction of IFN-α in peripheral blood dendritic cells by enveloped RNA and DNA viruses. *J. Immunol.* 161: 2391–2399.
33. Badley, A. D., A. A. Pilon, A. Landay, and D. H. Lynch. 2000. Mechanisms of HIV-associated lymphocyte apoptosis. *Blood* 96: 2951–2964.
34. Drenou, B., L. Amiot, N. Setterblad, S. Taque, V. Guilloux, D. Charron, R. Fauchet, and N. Mooney. 2005. MHC class II signaling function is regulated during maturation of plasmacytoid dendritic cells. *J. Leukocyte Biol.* 77: 560–567.
35. Fernandes-Alnemri, T., G. Litwack, and E. Alnemri. 1994. CPP32, a novel human apoptotic protein with homology to *Caenorhabditis elegans* cell death protein Ced-3 and mammalian interleukin-1β-converting enzyme. *J. Biol. Chem.* 269: 30761–30764.
36. Krutzik, P. O., M. R. Clutter, and G. P. Nolan. 2005. Coordinate analysis of murine immune cell surface markers and intracellular phosphoproteins by flow cytometry. *J. Immunol.* 175: 2357–2365.
37. Sato, M., H. Suemori, N. Hata, M. Asagiri, K. Ogasawara, K. Nakao, T. Nakaya, M. Katsuki, S. Noguchi, N. Tanaka, and T. Taniguchi. 2000. Distinct and essential roles of transcription factors IRF-3 and IRF-7 in response to viruses for IFN-α/β gene induction. *Immunity* 13: 539–548.
38. Barnes, B. J., P. A. Moore, and P. M. Pitha. 2001. Virus-specific activation of a novel interferon regulatory factor, IRF-5, results in the induction of distinct interferon-α genes. *J. Biol. Chem.* 276: 23382–23390.
39. Takauji, R., S. Iho, S. Takatsuka, T. Yamamoto, H. Takahashi, H. Kitigawa, R. Iwasakei, T. Iida, T. Yokochi, and T. Matsuki. 2002. CpG-DNA-induced IFN-α production involves p38 MAPK-dependent STAT-1 phosphorylation in human plasmacytoid dendritic cell precursors. *J. Leukocyte Biol.* 72: 1011–1019.
40. Rubio, G., X. Ferez, M. Sanchez-Campillo, J. Galvez, S. Marti, R. Verdu, T. Hernandez-Caselles, and P. Garcia-Penarrubia. 2004. Cross-linking of MHC class I molecules on human NK cells inhibits NK cell function, segregates MHC I from the NK cell synapse, and induces intracellular phosphotyrosines. *J. Leukocyte Biol.* 76: 116–124.
41. Al-Daccak, R., N. Mooney, and D. Charron. 2004. MHC class II signaling in antigen-presenting cells. *Curr. Opin. Immunol.* 16: 108–113.
42. Chieppa, M., G. Bianchi, A. Doni, A. Del Prete, M. Sironi, G. Laskarin, P. Monti, L. Piemonti, A. Biondi, A. Mantovani, et al. 2003. Cross-linking of the mannose receptor on monocyte-derived dendritic cells activates an anti-inflammatory immunosuppressive program. *J. Immunol.* 171: 4552–4560.
43. Elkord, E., P. E. Williams, H. Kynaston, and A. W. Rowbottom. 2005. Human monocyte isolation methods influence cytokine production from in vitro generated dendritic cells. *Immunology* 114: 204–212.
44. Blomberg, S., M. Eloranta, M. Magnuson, G. Alm, and L. Ronnblom. 2003. Expression of the markers BDCA-2 and BDCA-4 and production of interferon-α by plasmacytoid dendritic cells in systemic lupus erythematosus. *Arthritis Rheum.* 48: 2524–2532.
45. Kohrgruber, N., N. Halanek, M. Groger, D. Winter, K. Rappersberger, M. Schmitt-Egenolf, G. Stingl, and D. Maurer. 1999. Survival, maturation, and function of $CD11c^-$ and $CD11c^+$ peripheral blood dendritic cells are differentially regulated by cytokines. *J. Immunol.* 163: 3250–3259.
46. Marie, I., J. E. Durbin, and D. E. Levy. 1998. Differential viral induction of distinct interferon-α genes by positive feedback through interferon regulatory factor-7. *EMBO J.* 17: 6660–6669.
47. Caillaud, A., A. Prakash, E. Smith, A. Masumi, A. G. Hovanessian, D. E. Levy, and I. Marie. 2002. Acetylation of interferon regulatory factor-7 by p300/CREB-binding Protein (CBP)-associated factor (PCAF) impairs its DNA binding. *J. Biol. Chem.* 277: 49417–49421.
48. Sato, M., T. Taniguchi, and N. Tanaka. 2001. The interferon system and interferon regulatory factor transcription factors- studies from gene knockout mice. *Cytokine Growth Factor Rev.* 12: 133–142.